Syngeneic bone marrow transplantation in combination with PI3K inhibitor reversed hyperglycemia in later-stage streptozotocin-induced diabetes

Shiyun Zhang[1#], Qianqian Dai[1#], Bin Zhang[1#], Siyang Liu[1], Ying Wang[1], Yixue Zhang[1], Dongyue Chen[1], Ningning Zong[1], Hongwei Wang[1], Jingjing Ding[2], Qian Gao[1], Yanting Wen[1^]

[1]Department of Basic Medicine, Center of Translational Medicine, Jiangsu Key Laboratory of Molecular Medicine, Nanjing University Medical School, Nanjing, China; [2]Department of Respiratory Medicine, Jiangsu Key Laboratory of Molecular Medicine, the Affiliated Drum Tower Hospital of Nanjing University Medical School, Nanjing, China

Contributions: (I) Conception and design: Y Wen; (II) Administrative support: Y Wen, Q Gao, J Ding; (III) Provision of study materials or patients: S Zhang, Q Dai, B Zhang; (IV) Collection and assembly of data: S Zhang, Q Dai, B Zhang, S Liu, Y Wang, Y Zhang, D Chen, N Zong, H Wang; (V) Data analysis and interpretation: S Zhang, Q Dai, B Zhang; (VI) Manuscript writing: All authors; (VII) Final approval of manuscript: All authors.
[#]These authors contributed equally to this work.

Correspondence to: Yanting Wen; Qian Gao. Center of Translational Medicine, Jiangsu Key Laboratory of Molecular Medicine, Nanjing University Medical School, Nanjing 210093, China. Email: wenyanting@nju.edu.cn; qian_gao@nju.edu.cn; Jingjing Ding. Respiratory Medicine, Jiangsu Key Laboratory of Molecular Medicine, the Affiliated Drum Tower Hospital of Nanjing University Medical School, Nanjing 210093, China. Email: dingflower@hotmail.com.

Background: Type 1 diabetes (T1D) is a multiple factor autoimmune disease characterized by T cell-mediated immune destruction of islet β cells. Autologous hematopoietic stem cell transplantation (AHSCT) has been a novel strategy for patients with new-onset T1D, but not for those with a later diagnosis. Disturbance of regulatory T cells (Tregs) likely contributes to poor response after transplantation in later-stage T1D. Inhibition of phosphoinositide 3-kinases (PI3K)/Akt signaling maintains Tregs' homeostasis.

Methods: We built a later-stage streptozotocin (STZ)-induced T1D mouse model. Syngeneic bone marrow transplantation (syn-BMT) was performed 20 days after the onset of diabetes in combination with BKM120 (a PI3K inhibitor). Meanwhile, another group of STZ-diabetic mice were transplanted with bone marrow cells cocultured with BKM120 *in vitro* for 24 h. Fasting glucose and glucose tolerance were recorded during the entire experimental observation after syn-BMT. Samples were collected 126 days after syn-BMT. Hematoxylin and eosin (H&E) staining was used to detect the effect of PI3K inhibitor combined with syn-BMT on morphology of the T1D pancreas. CD4+CD25− T cells and CD4+CD25+ T cells were sorted by magnetic cell sorting (MACS), then fluorescence activated cell sorting (FACS) and quantitative real-time PCR (qPCR) were used to detect the effect of PI3K inhibitor on modulating immune disorder and restoring the function of Treg cells.

Results: Our investigation showed syn-BMT in combination with BKM120 effectively maintained normoglycemia in later-stage T1D. The disease remission effects may be induced by the rebalance of Th17/Tregs dysregulation and restoration of Tregs' immunosuppressive function by BKM120 after syn-BMT.

Conclusions: These results may reveal important connections for PI3K/Akt inhibition and Tregs' homeostasis in T1D after transplantation. AHSCT combining immunoregulatory strategies such as PI3K inhibition may be a promising therapeutic approach in later-stage T1D.

Keywords: Type 1 diabetes (T1D); syngeneic bone marrow transplantation (syn-BMT); BKM120; phosphoinositide 3-kinases (PI3K)/Akt signaling; regulatory T cells (Tregs)

Page 2 of 15

Zhang et al. Syngeneic BMT and PI3K inhibitor reversed later-stage T1D

Introduction

Type 1 diabetes (T1D) is an autoimmune disease characterized by T cell-mediated self-destruction of insulin-secreting islet β cells and resultant hyperglycemia (1,2). Insulin remains the mainstay of therapy, while pramlintide is the only non-insulin medication approved for improved glycemic control for T1D patients. Despite these managements, the disease continues to be associated with substantial complications, including retinopathy, neuropathy, nephropathy, neurocognitive disorders, as well as atherosclerosis and thrombosis in the heart, peripheral arteries, and brain (1,3).

Novel strategies that focus on suppressing autoimmunity and preserving β cells in T1D, such as autologous hematopoietic stem cell transplantation (AHSCT) (4-9), have opened the door to new therapeutic approaches. AHSCT for new-onset T1D (within 6 weeks of diagnosis) can prevent 82% of the patients from insulin dependence, compared with 40% of the cases whose treatment was initiated at a later time point (10). Indeed, to be an effective therapy, AHSCT needs to be performed earlier in the time course of T1D. This unique challenge makes it difficult to translate the therapeutic potential of AHSCT to clinic.

We previously reported that for getting a promising therapy from syngeneic bone marrow transplantation (syn-BMT) for T1D, an early time window should be chosen in streptozotocin (STZ)-diabetic mice. syn-BMT, performed when T1D was new-onset (10 days), was safe and able to reverse the diabetic status, but could only attenuate diabetes at a later stage (20 or 40 days after onset). It was also revealed that the regeneration of regulatory T cells (Tregs) may correlate with the possible prolonged remission-induction introduced by syn-BMT (11,12). Treg plays a critical role in maintaining peripheral tolerance to self-antigens, thereby controlling autoimmunity, limiting immune responses to foreign antigens and suppressing exaggerated immune responses (13). Herein, we sought to determine whether syn-BMT combined with BKM120, a phosphoinositide 3-kinases (PI3K) inhibitor which we have harnessed for introducing optimal Treg responses in a mouse model of pulmonary sarcoidosis (14), could improve the diabetic-remission-inducing effects of syn-

BMT in STZ-induced T1D animals at a later stage. Our data indicate that syn-BMT in combination with BKM120 conferred protection from immune attack, controlled blood glucose in later-stage STZ-induced T1D, and maintained Treg homeostasis and function. We present the following article in accordance with the ARRIVE reporting checklist (available at https://dx.doi.org/10.21037/atm-21-3329).

Methods

Mice

Four- to six-week-old male C57BL/6 mice were purchased from the Sino-British SIPPR/BK Lab Animal Ltd. (Shanghai, China). Mice were housed under specific-pathogen-free conditions for one week. All experimental protocols were approved under a project license (SCXK-Jiangsu-2019-0056) granted by Institutional Animal Care and Use Committee of Nanjing University, in compliance with institutional guidelines for the care and use of animals.

Induction of T1D and bone marrow cell transplantation

T1D was induced by intraperitoneal injection with 40 mg/kg STZ (Sigma, St. Louis, MO, USA) dissolved in 0.1 mL chilled sodium citrate buffer (pH 4.2 to 4.5) for 5 consecutive days. Blood samples were collected from the tail vein after fasting, and diabetic status was determined with blood glucose monitor (Sinocare, Changsha, China). Mice were considered diabetic when glycemia was >13.9 mmol/L (250 mg/dL) after two consecutive determinations. Mice injected with 0.1 mL citrate buffer were used as control (group Normal). After syn-BMT, fasting blood glucose (FBG) was monitored weekly for 126 days.

Bone marrow cell transplantation and experimental groups

Donor C57BL/6 male mice were euthanized, and bone marrow cells from femur and tibia were collected into ice-cold PBS. Single bone marrow cells were obtained by filtration through a 75-μm filter. For erythrocyte depletion, cells were treated with lysis buffer (0.15 M NH_4Cl,

1 mM $KHCO_3$, and 0.1 mM Na_2-EDTA, pH 7.4), and resuspended in RPMI-1640 (GIBCO) (containing 10% FCS, 100 U/mL penicillin and 100 μg/mL streptomycin). Concentration was adjusted to 2×10^7 cells/mL. Parts of these cells were cocultured with 5 μM BKM120 for 24 h at 37 ℃ in 5% CO_2.

T1D mice were randomly divided into 4 groups, including T1D mice group (group T1D), mice that received syn-BMT only (group syn-BMT), mice that received syn-BMT together with intravenous injection of BKM120 (group syn-BMT + BKM120), and mice transplanted with syngeneic bone marrow cells cocultured with BKM120 for 24 h (group syn-BMT + BKM120-24 h) (*Figure 1A*).

syn-BMT was performed on day 20 after diabetes onset. As the recipient, T1D mice were irradiated in a total of 800 cGy (from a ^{60}Co source, 0.95–1 Gy/min). Ten million prepared bone marrow cells were intravenously injected into each recipient 6 h after irradiation. Thereafter, recipients were provided with antibiotic water containing 2 mg/mL neomycin sulfate for at least 3 weeks. A protocol was prepared before the study without registration.

Intraperitoneal glucose tolerance test (IPGTT)

IPGTTs were carried out on day 110 after transplantation. Mice were intraperitoneally injected with 10% glucose at a dosage of 2 g/kg after 8 h of fasting. Blood glucose was detected before injection and at 30, 60, 90 and 120 min, respectively, after the injection.

Fluorescence activated cell sorting (FACS)

Mice were euthanized on the 126th day. Spleens, inferior epigastric lymph nodes and mesenteric lymph nodes were collected and single-cell suspensions were then obtained from mononuclear cells (MNCs). Cells were stained with fluorescent surface antibodies: FITC-conjugated Anti-Mouse CD4, APC-conjugated Anti-mouse CD8a, FITC-conjugated Anti-mouse CD11b, FITC-conjugated Anti-mouse CD11c, APC-conjugated Anti-mouse Gr-1, APC-conjugated Anti-mouse MHCII (all from BD Biosciences, San Jose, CA, USA). For staining of cytokines: APC-conjugated Anti-mouse IFNγ, PE-conjugated Anti-Mouse IL-4 and PE-conjugated Anti-Mouse IL-17A were purchased from BD Biosciences. Mouse regulatory T cell staining kit (eBioscience, San Diego, CA, USA) was used according to the manufacturer's instructions. For intracellular cytokine staining, cells were restimulated with Cell Stimulation Cocktail (BD Biosciences) for 4 h at 37 ℃. Cell phenotyping and sorting were performed on a BD FACS Calibur system (BD Biosciences) and data were analyzed using FlowJo software.

Immunosuppression assay of Treg

$CD4^+CD25^+$ T cells were isolated from MNCs using microbeads magnetic separation provided by magnetic cell sorting (MACS) (Miltenyi Biotec, Germany) and $CD4^+CD25^-$ T cells [effector T cell (Teff)] were meanwhile collected from group Normal. To measure cell proliferation, sorted $CD4^+CD25^+$ T cells were co-cultured with carboxyfluorescein succinimidyl ester (CFSE)-labeled $CD4^+CD25^-$ T cells (1×10^6) at the ratio of 3:1 or 1:1 in RPMI-1640 containing 10% fetal bovine serum (Thermo Fisher Scientific, Waltham, MA, USA) in the presence of IL-2 (1 μg/1×10^6 cells) and anti-CD3/CD28 antibodies (1 μg/1×10^6 cells) using 12 well plates at 37 ℃ for 72 h. FACS was used to delineate the ratio of CFSE + cells.

Quantitative real-time PCR (qPCR)

Total RNA was isolated from MNCs derived from lymph nodes using RNAisoPlus reagent (Takara, Kusatsu, Japan). RNA was reverse-transcribed into cDNA using HiScript III RT SuperMix for qPCR (Vazyme Biotech, Nanjing, China) as manufacturer's protocols. qPCR reactions for each cDNA sample were performed with ChamQ Universal SYBR Q-PCR Master Mix (Vazyme Biotech) in a Viia7 Real-Time PCR System (Applied Biosystems, Waltham, MA, USA). The gene specific primers utilized for qPCR assays were shown in *Table 1*. PCR procedures were as follows: 95 ℃ for 10 min followed by 40 cycles at 95 ℃ for 15 s, 60 ℃ for 1 min, 72 ℃ for 30 s. qPCR data for each target gene were normalized to GAPDH and were expressed as $2^{-\Delta\Delta Ct}$. Each sample was analyzed in triplicate.

Pancreata morphometry and immunofluorescence

Pancreata were dissected from each group and fixed in 10% formalin and paraffin embedded. To assess the islet morphology, paraffin-sections (2 mm thickness) were cut 3 μm apart from blocks and stained with hematoxylin and eosin (H&E). Conventional morphological evaluation was performed under light microscope (Olympus, Tokyo, Japan). After dewaxing, rehydration and heat-induced

Page 4 of 15

Zhang et al. Syngeneic BMT and PI3K inhibitor reversed later-stage T1D

Table 1 The primer sequences

Primer	Forward	Reverse
T-bet	TGCCCGAACTACAGTCACGAAC	AGTGACCTCGCCTGGTGAAATG
IL-6	AGACTTCCATCCAGTTGCCTTCTTG	GCCTCCGACTTGTGAAGTGGTATAG
RORγt	TACCTTGGCCAAAACAGAGG	GATGCCTGGTTTCCTCAAAA
FoxP3	GGCCCTTCTCCAGGACAGA	GCTGATCATGGCTGGGTTGT
TGF-β1	ACCATGCCAACTTCTGTCTG	CGGGTTGTGTTGGTTGTAGA
IL-17	TTTAACTCCCTTGGCGCAAAA	CTTTCCCTCCGCATTGACAC
IL-23	TGGCATCGAGAAACTGTGAGA	TCAGTTCGTATTGGTAGTCCTGTTA
IL-33	TCCAACTCCAAGATTTCCCCG	CATGCAGTAGACATGGCAGAA
STAT3	CCAAGTTCATCTGTGTGACACC	ATCGGCAGGTCAATGGTATTGC
GAPDH	CTGGTGCTGCCAAGGCTGTG	TCTCCAGGCGGCACGTCAG

IL, interleukin; RORγt, retinoid-related orphan receptor γ; FoxP3, fork head box protein P3; TGF-β, transforming growth factor β; STAT3, signal transducer and activator of transcription 3; GAPDH, glyceraldehyde-3-phosphate dehydrogenase.

antigen retrieval treatment, sections were incubated in blocking solution, then stained with Phosphorylation-PI3K p85α (Tyr458) polyclonal antibody and Phosphorylation-Akt (Ser473) Rabbit monoclonal antibody (Cell Signaling Technology, Danvers, MA, USA) overnight at 4 ℃ and Alexa fluor 488 AffiniPure goat anti-rabbit IgG and Alexa fluor 647 AffiniPure goat anti-rabbit IgG (Fcmacs Biotech Co., Nanjing, China) for 1.5 h. DAPI (4',6-diamidino-2-phenylindole, Beyotime Biotechnology, Shanghai, China) was added at 1 μg/mL to the secondary antibody solution. For immunofluorescence assay, slides were visualized with FV3000 confocal microscope (Olympus, Tokyo, Japan).

Western blot

Total protein was extracted from pancreas or Treg separated from spleen by using radio immunoprecipitation assay buffer (RIPA) containing 0.1% sodium dodecyl sulfate (SDS). Protein from each sample was separated on 10% Tris-Tricine SDS-PAGE gel and transferred to polyvinylidene fluoride membranes, and blotted with appropriate antibodies. PI3K p85α (6G10) mouse monoclonal antibody, Phosphorylation-PI3K p85α (Tyr458)/p55 (Tyr199) antibody, Phosphorylation-Akt (Ser473) Rabbit monoclonal antibody were purchased from Cell Signaling Technology. Human/Mouse/Rat Akt pan specific monoclonal antibody (Bioworld Technology, Minneapolis, MN, USA). β-Actin Rabbit polyclonal antibody (Bioworld Technology) was used as internal control.

Statistical analyses

Data were analyzed by one-way analysis of variance (ANOVA). Statistical analyses and graphs were made by using GraphPad Prism 8 (GraphPad Software). Data were expressed as means ± SEM. Differences between cohorts were assessed using Student's t-test or Tukey's test. $P<0.05$ was considered statistically significant.

Results

syn-BMT combined with BKM120 administration ameliorated blood glucose in STZ-induced T1D

To evaluate the effect of syn-BMT combined with BKM120 on diabetic mice, four groups were analyzed in later-stage (20 days) STZ-diabetic mice: group syn-BMT received syn-BMT only, group syn-BMT + BKM120 received syn-BMT together with intravenous injection of BKM120, group syn-BMT + BKM120-24 h was transplanted with syngeneic bone marrow cells that were cocultured with BKM120 for 24 h before usage, and group T1D received no treatment. Group Normal was normal mice (shown in *Figure 1A*). In the whole experimental period (126 days after BMT), group T1D had a diminished survival rate of 66.7% (8/12), whereas no death was observed in the other groups.

Throughout the entire experimental period of 126 days, the FBG of group T1D was, as expected, at a gradually higher level. The glucose tolerance test on day 110 showed that compared with group T1D, group syn-BMT had
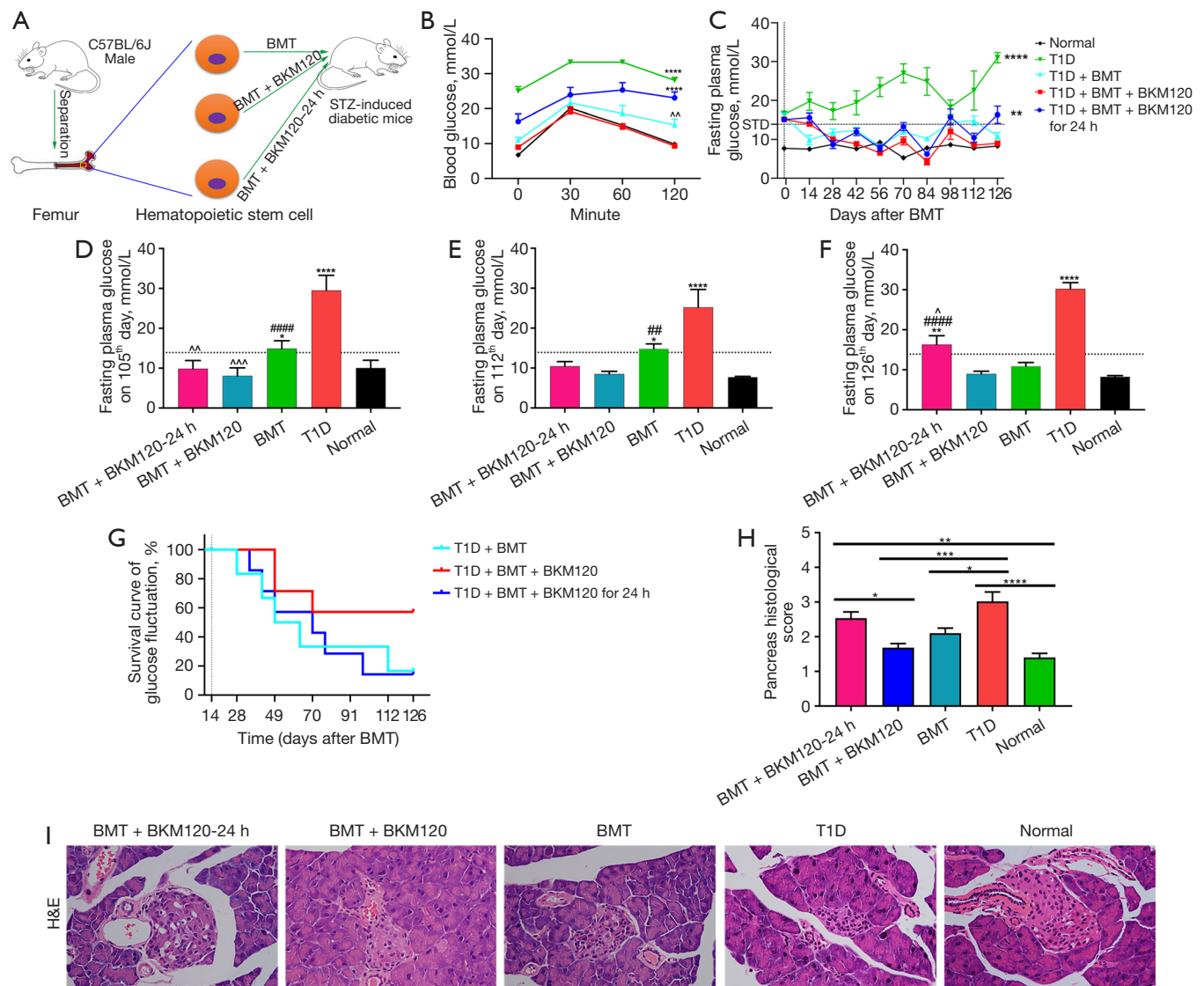
Figure 1 Treatment with BKM120 reduced the inflammation resulting from syn-BMT. Male C57BL/6J mice were induced with 40 mg/kg STZ by intraperitoneal injection for 5 consecutive days. Hematopoietic stem cells were separated from the femur of allogeneic male mice. The separated hematopoietic stem cells were treated with 5 mg/kg BKM120 *in vitro* and/or transplanted with hematopoietic stem cells without any treatment. All the mice were sacrificed on 126th day after transplantation. (B) Blood glucose tolerance test and (C) fasting plasma glucose test was performed on day 120 after syn-BMT of BKM120 treatment T1D mice after syn-BMT *in vivo* and *in vitro* and without treatment. (D) Fasting plasma glucose on day 105, (E) 112 and (F) 126. (G) Survival curve of glucose fluctuation after syn-BMT. (H) Pancreas histological scores according to H&E stain of pancreas sections. (I) Representative H&E stain of pancreas sections from each group (magnification, ×400). N≥5 for each group. *, P<0.05; **, P<0.01; ***, P<0.001; ****, P<0.0001; ^, P<0.05; ^^, P<0.01; ^^^, P<0.001; ##, P<0.01; ####, P<0.0001; #, compared with group T1D; ^, compared with group syn-BMT. T1D, type 1 diabetes; STZ, streptozotocin; syn-BMT, syngeneic bone marrow transplantation; H&E, hematoxylin and eosin.

improved glucose tolerance, while group syn-BMT + BKM120-24 h did not show statistical improvement. In contrast, group syn-BMT + BKM120 had a response similar to the normal mice (*Figure 1B,1C*). The FBG in groups syn-BMT, syn-BMT + BKM120 and syn-BMT + BKM120-24 h, on the other hand, dropped significantly on day 28

Page 6 of 15

Zhang et al. Syngeneic BMT and PI3K inhibitor reversed later-stage T1D

after the indicated treatments and remained close to the normoglycemia for another 28 days (*Figure 1C*). After that, the FBG in groups syn-BMT and syn-BMT + BKM120-24 h fluctuated, and relapsed to hyperglycemia on days 98 and 126 in group syn-BMT + BKM120-24 h, and on days 98, 105 and 112 in group syn-BMT (*Figure 1C-1F*). Notably, the glucose fluctuation (measured as the first single test of FBG >13.9 mmol/L and then decreased again) occurred much less and later in group syn-BMT + BKM120, and the animals in this group remained a relatively steady normoglycemia during the whole experimental period (*Figure 1C,1G*). Pancreata histological examination on experimental day 126 showed that compared with normal mice, the number of destroyed islets in T1D mice was increased. Whereas, the size and integrity of the islets in groups syn-BMT and syn-BMT + BKM120 were largely normal, better than group syn-BMT + BKM120-24 h, when compared to those in group T1D (*Figure 1H,1I*). Together, BKM120 improved the effect of syn-BMT in controlling blood glucose in later-onset STZ-induced T1D.

BKM120 improved immune derangement after syn-BMT in STZ-induced T1D

CD4⁺/CD8⁺ T cells

To detect the immunomodulatory status of helper/cytotoxic T cells, we measured the frequencies of CD4⁺ and CD8⁺ T cells isolated from inferior epigastric lymph nodes on day 126 after syn-BMT. The proportions of CD4⁺CD8⁻ T cells in groups syn-BMT, syn-BMT + BKM120 and syn-BMT + BKM120-24 h were higher than that in group T1D (37.23%±8.531%, 47.57%±3.355% and 35.33%±1.581% *vs.* 15.99%±3.794%; P=0.0217, P=0.0004 and P=0.0423, respectively), whereas CD4⁻CD8⁺ T cells in group syn-BMT + BKM120 decreased (13.81%±2.379% *vs.* 31.90%±4.755%, P=0.0407). Comparable with Normal and T1D groups, the proportion of CD4⁻CD8⁺ T cells in group syn-BMT + BKM120-24 h was lower (8.77%±1.075% *vs.* 27.64%±0.893% and 31.9%±4.755%; P=0.0431 and P=0.0055, respectively) (*Figure 2A*).

Th1/Th2

We also noticed that the proportions of Th1 (CD4⁺IFNγ⁺ T cells) in groups T1D and syn-BMT were significantly higher than that in group Normal (9.215%±0.912% and 10.68%±1.841% *vs.* 2.79%±0.549%; P=0.0005 and P<0.0001, respectively), while those in groups syn-BMT + BKM120 and syn-BMT + BKM120-24 h both decreased significantly

while being compared with group T1D (1.486%±0.495% and 4.268%±0.373% *vs.* 9.215%±0.912%; P<0.0001 and P=0.0108, respectively) or group syn-BMT (1.486%±0.495% and 4.268%±0.373% *vs.* 10.68%±1.841%; P=0.0006 and P=0.02, respectively). Concerning Th2 (CD4⁺IL-4⁺ T cells), there was a significant increase in group syn-BMT + BKM120-24 h in comparison with that in group T1D or syn-BMT + BKM120 (13.34%±4.115% *vs.* 3.922%±0.5459% and 1.909%±0.5258%; P=0.0282 and P=0.0086, respectively) (*Figure 2B*).

MDSCs/DCs

We went on to determine the changes in MDSCs and DCs, the major immune modulators, isolated from the mesenteric lymph nodes and spleens of different groups. We noticed that CD11b⁺Gr-1⁺ cells derived from mesenteric lymph nodes significantly increased in group syn-BMT + BKM120 in comparison with group Normal, group T1D and group syn-BMT (1.822%±0.366% *vs.* 0.8302%±0.0889%, 0.689%±0.0606%, and 0.871%±0.2083%; P=0.0122, P=0.0039 and P=0.0243, respectively). Meanwhile, CD11b⁺Gr-1⁺ cells in the spleen in group syn-BMT were down-regulated compared with group control or group T1D (0.3392%±0.06924% *vs.* 1.235%±0.2151% and 1.514%±0.291%; P=0.0355 and P=0.0041, respectively), while those in group syn-BMT + BKM120 were preserved (*Figure 2C*).

Furthermore, while CD11c⁺MHCII⁺ cells derived from mesenteric lymph nodes in group syn-BMT showed a statistical decrease compared with group T1D (0.5058%±0.0748% *vs.* 1.55%±0.2282%, P=0.0148), they were greatly increased in group syn-BMT + BKM120 when compared with group syn-BMT and group syn-BMT + BKM120-24 h (1.722%±0.2523% *vs.* 0.5058%±0.0748%, and 0.672%±0.1838%; P=0.0037 and P=0.0141, respectively). Similar results were observed in CD11c⁺MHCII⁺ cells isolated from the spleens (*Figure 2D*).

Th17/Treg

There was no statistical difference in the frequencies of Th17 and Treg isolated from mesenteric lymph nodes between groups T1D and control. Increased numbers of Th17 have been found in association with syn-BMT compared with groups control and T1D (12.48%±0.4488% *vs.* 7.248%±0.8302% and 8.126%±1.280%; P=0.0053 and P=0.0236, respectively), whereas Th17 in groups syn-BMT + BKM120 and syn-BMT + BKM120-24 h was significantly down-regulated in comparison with group syn-BMT (5.880%±0.8645% and 4.288%±0.9720% *vs.* 12.48%±0.4488%; P=0.0005 and P<0.0001, respectively)
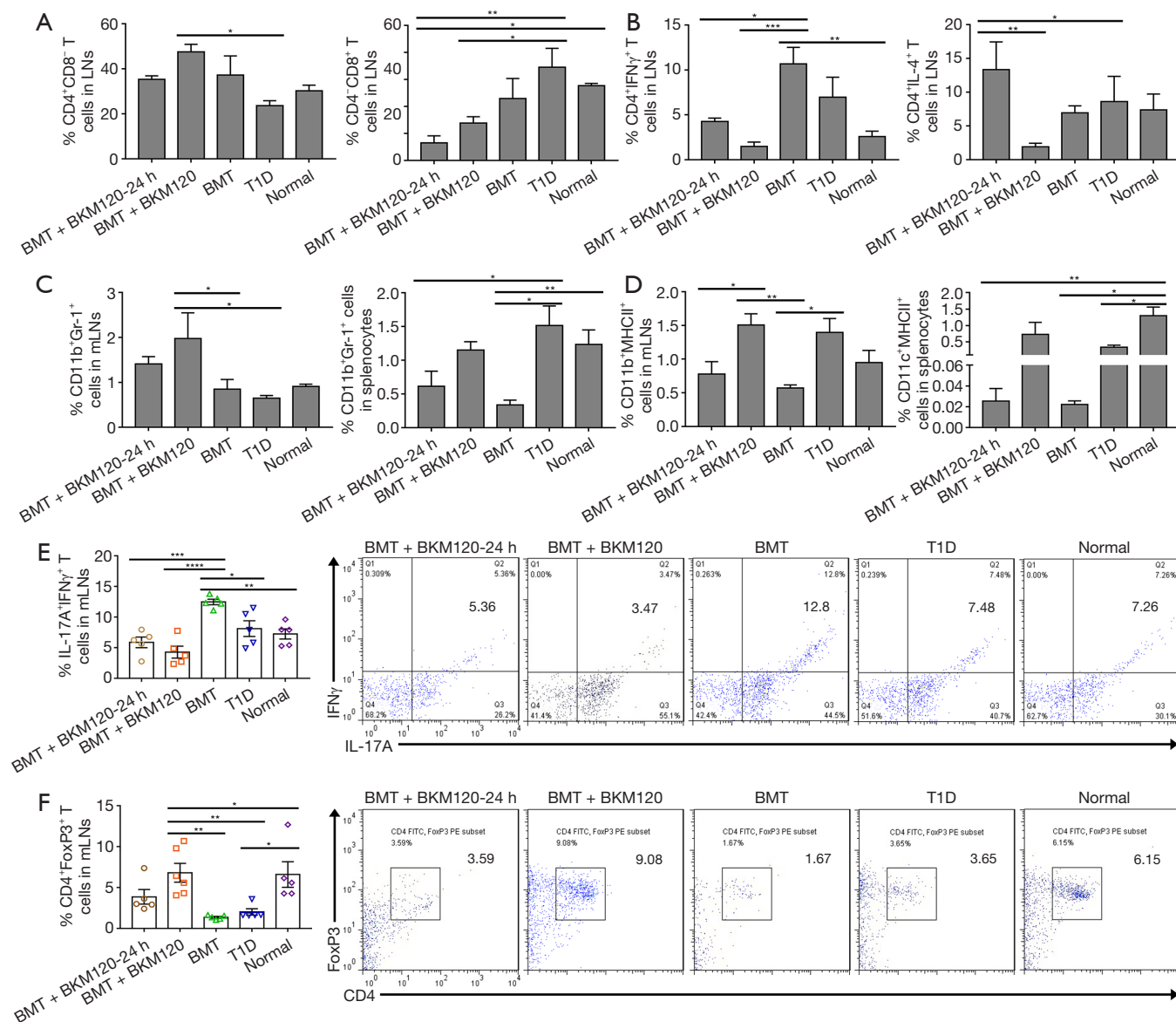
Figure 2 BKM120 restored the balance of Th17 and Treg caused by syn-BMT. Percentages of CD4+CD8− T cells and CD4−CD8+ T cells, (B) CD4+IFNγ+ T cells and CD4+IL-4+ T cells were isolated from inferior epigastric lymph nodes of each group and analyzed by FACS. (C) Percentages of CD11b+Gr1+ cells and (D) CD11c+MHCII+ cells were separated from mesenteric lymph nodes and spleen of each group. (E) Percentages of IL-17A+IFNγ+ T cell and (F) CD4+FoxP3+ T cells and in mesenteric lymphocytes of each group. N≥5 for each group. *, P<0.05; **, P<0.01; ***, P<0.001; ****, P<0.0001. T1D, type 1 diabetes; IL, interleukin; IFNγ, interferon gamma; FACS, fluorescence activated cell sorting; MHC, major histocompatibility complex; FoxP3, fork head box protein P3.

(*Figure 2E*). Meanwhile, we found lower frequencies of Treg in group T1D and group syn-BMT compared with group control (1.848%±0.2084% and 1.413%±0.1017% *vs.* 6.602%±1.568%; P=0.0184 and P=0.0061, respectively), while the frequency increased significantly in group syn-BMT + BKM120 when compared with group T1D

(6.828%±1.147% *vs.* 1.848%±0.2084%, P=0.0026) (*Figure 2F*). Notably, there was no significant improvement in Treg cells in group syn-BMT + BKM120-24 h.

Though the relative expression of mRNA for *T-bet* showed no difference between group Normal and group T1D, it statistically increased in group syn-BMT + BKM120-
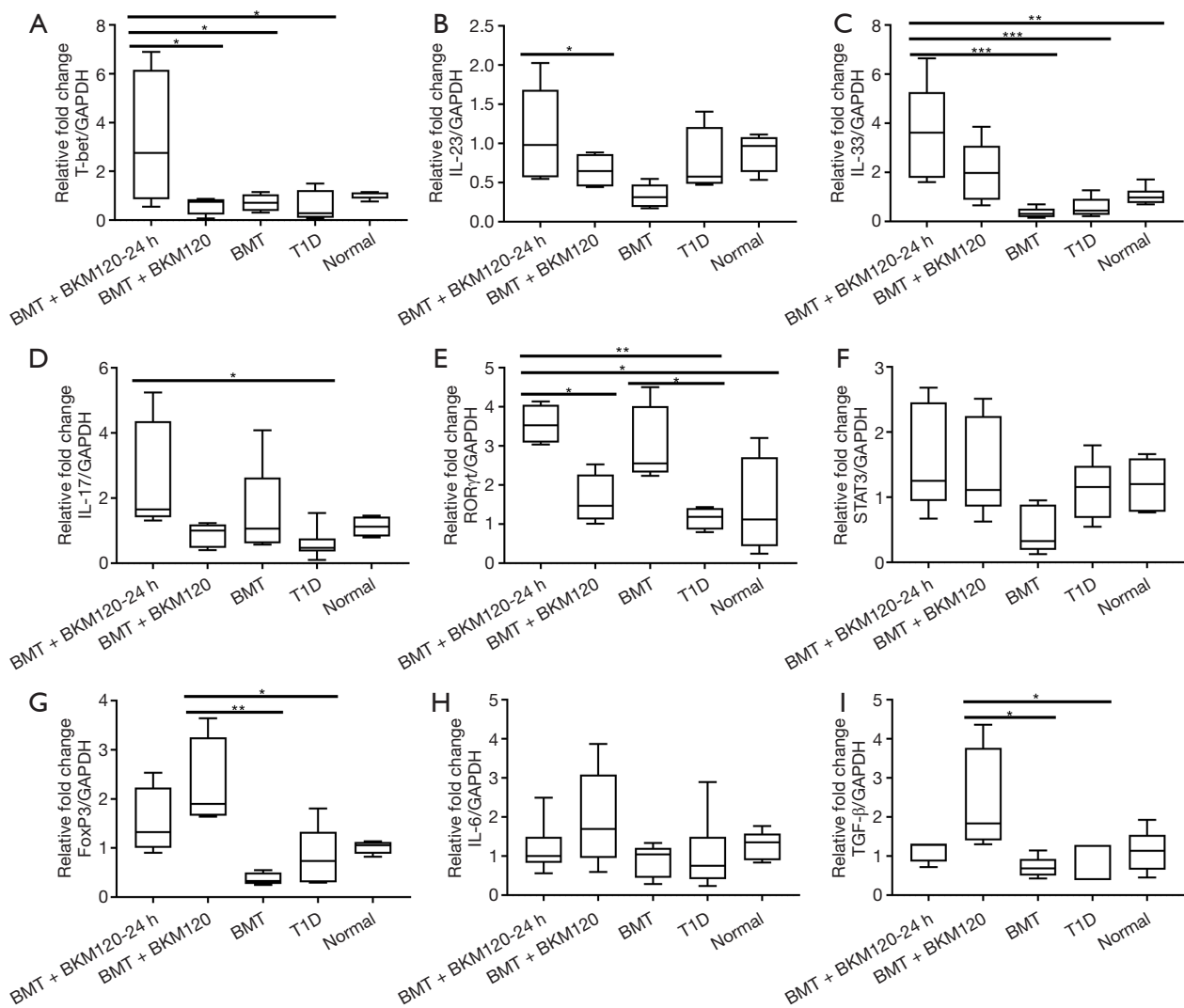
Page 8 of 15

Zhang et al. Syngeneic BMT and PI3K inhibitor reversed later-stage T1D

Figure 3 syn-BMT combined with BKM120 rebalanced immune disorders in STZ-induced T1D. Relative copies of (A) T-bet, (B) IL-23, (C) IL-33, (D) IL-17, (E) RORγt, (F) STAT3, (G) FoxP3, (H) IL-6 and (I) TGF-β mRNA isolated from MNCs derived from lymph nodes and were measured by real-time PCR. GAPDH was used as internal control. N=6 for each group. *, $P<0.05$; **, $P<0.01$; ***, $P<0.001$. GAPDH, glyceraldehyde-3-phosphate dehydrogenase; T1D, type 1 diabetes; syn-BMT, syngeneic bone marrow transplantation; STZ, streptozotocin; IL, interleukin; IFNγ, interferon gamma; RORγt, retinoid-related orphan receptor γ; STAT3, signal transducer and activator of transcription 3; FoxP3, fork head box protein P3; TGF-β, transforming growth factor β; MNCs, mononuclear cells; PCR, polymerase chain reaction.

24 h (*Figure 3A*) compared with that of group syn-BMT + BKM120 (P=0.0373, respectively). The expression of *ROR-γt* in groups syn-BMT and syn-BMT + BKM120-24 h showed remarkable increase in comparison with group T1D (P=0.0489 and P=0.0069; respectively). Meanwhile, IL-23, IL-33 and IL-17 increased significantly only in group syn-BMT + BKM120-24 h (*Figure 3B-3E*). In parallel, the expressions of fork head box protein P3 (FoxP3) and TGF-β

were significantly increased in group syn-BMT + BKM120 in comparison with group T1D (P=0.0147 and P=0.0206; respectively) and group syn-BMT (P=0.0028 and P=0.0171; respectively), while STAT3 and IL-6 seemed less sensitive (*Figure 3F-3I*). These results suggested the difference of an anti-inflammatory Treg from a pro-inflammatory Th17 phenotype between groups syn-BMT + BKM120 and syn-BMT + BKM120-24 h.

syn-BMT combined with BKM120 treatment restored the immunosuppressive function of Treg

Next, we asked whether the treatment of syn-BMT combined with BKM120 regulates the immunosuppressive function of Treg. After co-culturing $CD4^+CD25^+$ T cells with Teff at ratios of 1:1 and 3:1, the proliferated $CFSE^+$ T cells significantly increased both in group T1D (65.83%±2.21% and 71.97%±2.294% *vs.* 24.70%±4.082%; P<0.0001 and P<0.0001, respectively) and group syn-BMT (73.78%±1.766% and 81.13%±3.371% *vs.* 39.53%±5.845%; P<0.0001 and P<0.0001, respectively) compared with group Normal. Interestingly, treatments of syn-BMT + BKM120 significantly reversed these increases [31.52%±5.539% *vs.* 71.97%±2.294%, P<0.0001 (Treg:Teff =1:1); 49.85%±4.148% *vs.* 81.13%±3.371%, P<0.0001 (Treg:Teff =3:1)], whereas syn-BMT + BKM120-24 h did not, indicating that BKM120 administered in recipients in combination with syn-BMT recovered the immunosuppressive function of Treg in STZ-diabetic mice (*Figure 4A,4B*).

BKM120 reversed excessive activation of PI3K/Akt signaling by syn-BMT

We next detected the activation of PI3K/Akt signaling pathway in pancreas and Treg. As shown in *Figure 5*, in the normal pancreas, both PI3K and Akt were activated with regional variations judged by an immunofluorescence staining. Compared with group Normal, in the pancreas in group T1D, both P-PI3K and P-Akt staining were significantly reduced, whereas in group syn-BMT, they were significantly and broadly increased, suggesting that the BMT performance strongly triggered the pathway. Importantly, this activation of PI3K/Akt signaling by syn-BMT was largely reversed in the pancreas in groups syn-BMT + BKM120 and syn-BMT + BKM120-24 h (*Figure 5A,5B*).

As to those in Treg isolated from the spleens, it was noted that in normal mice, PI3K was significantly activated, but not AKT. In contrast, in the Treg of group T1D, P-PI3K was down-regulated, while P-Akt was greatly up-regulated relative to the normal controls. It is not clear why and how the activation of PI3K/Akt was not synchronized. Importantly, syn-BMT treatment significantly stimulated both, whereas both syn-BMT + BKM120 and syn-BMT + BKM120-24 h effectively reversed this activation of PI3K/Akt signaling in Treg (*Figure 5C*). Collectively, these data demonstrated that BKM120 contributed to the suppression of the aberrant activation of PI3K/Akt signaling in both pancreas and Treg by syn-BMT, and may thus deliver beneficial effect in later-stage STZ-induced diabetes.

Discussion

Defective numbers or functions of Treg have been associated with chronic activation of the immune system (13). There have been advances in our understanding that the control of PI3K/Akt/mTOR cascade in Treg is critical for maintaining their homeostasis, suppressor function and stability (15-20). PI3K/Akt signaling contributes to the development and stability of natural and induced Treg. PI3K/Akt signals have been proven to prevent FOXO factors from localizing to the nucleus, Foxp3 expression and Treg transcriptional program, therefore antagonizing Treg development (18,21,22). The activation of PI3K/Akt signaling blocks FoxP3 expression, limits the anti-inflammatory effects of Treg, changes the metabolic programming of Treg, and declines in their stability (16,17,23,24).

The application of PI3K inhibitors as tolerance permissive drugs to enhance Treg expansion has been investigated. PI3Kδ inhibitors targeting Treg improved cancer immunotherapy (25). PI3Kγ inhibitor ameliorated TNBS-induced colitis by inhibiting multiple inflammatory components through the NF-κB pathway, and simultaneously inducing an increase in the functional activity of Treg (26). In addition, early administration of PI3Kγ inhibitor successfully suppressed effector T cells and the inflammatory cytokines produced by autoreactive T cells, induced Treg expansion through the cAMP response element-binding pathway, and therefore, reversed autoimmune diabetes in NOD mice (27). Equally encouraging, our previous results reported that BKM120 which inhibits all the four class I PI3K catalytic isoforms (p110α, β, γ and δ) (28), rebalanced Th1/Treg, inhibited the production of inflammatory cytokines, enhanced Treg's function and ameliorated granuloma in experimental pulmonary sarcoidosis (14). In addition, the metabolic regulation of insulin, the main regulatory hormone in energy metabolism of sugar and fat, is mainly mediated by PI3K/Akt signaling as well (29). In this regard, the PI3K pathway is an attractive target for the regeneration of Treg in later-stage T1D. Although PI3K inhibitors cannot improve blood glucose in STZ-diabetic mice (30), when Treg homeostasis may correlate with the possible prolonged remission-induction introduced by syn-BMT in STZ-induced T1D (11,12). Targeting PI3K along with syn-BMT
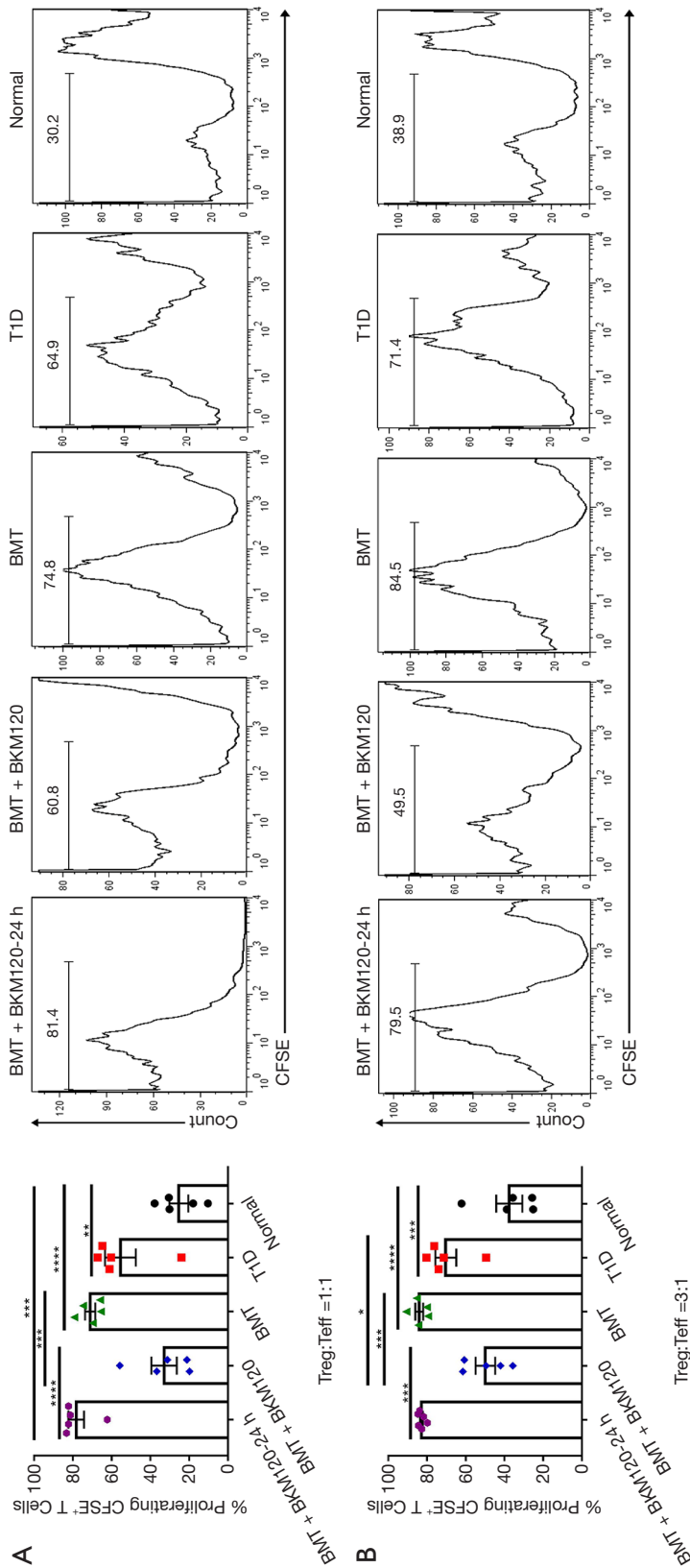
Page 10 of 15

Zhang et al. Syngeneic BMT and PI3K inhibitor reversed later-stage T1D

Figure 4 Inhibition of PI3K/Akt signaling pathway in Treg enhanced immunosuppressive function in STZ-induced T1D after syn-BMT. CD4⁺CD25⁺ T cells (Treg) and CD4⁺CD25⁻ T cells (Teff) were separated from spleen of each group by MACS. The frequency of CFSE⁺ labeled T cells in these cultures were analyzed by FACS. (A) CFSE labeled Treg co-cultured with Teff at the ratio of 1:1 for 72 hours in the presence of IL-2 and anti-CD3/CD28 antibodies. And the representative histograms depicting proliferated CFSE⁺ T cells when Treg and Teff were co-cultured at a ratio of 1:1 were showed. (B) CFSE labeled Treg was co-cultured with Teff at the ratio of 3:1 for 72 h in the presence of IL-2 and anti-CD3/CD28 antibodies. And the representative histograms depicting proliferated CFSE⁺ T cells when Treg and Teff were co-cultured at a ratio of 3:1 were showed. N=5 for each group. *, P<0.05; **, P<0.01; ***, P<0.001; ****, P<0.0001. T1D, type 1 diabetes; CFSE, carboxyfluoresce in succinimidyl ester; PI3K, phosphoinositide 3-kinases; Akt, protein kinase B; Treg, regulatory T cell; Teff, effector T cell; STZ, streptozotocin; FACS, fluorescence activated cell sorting; IL, interleukin.
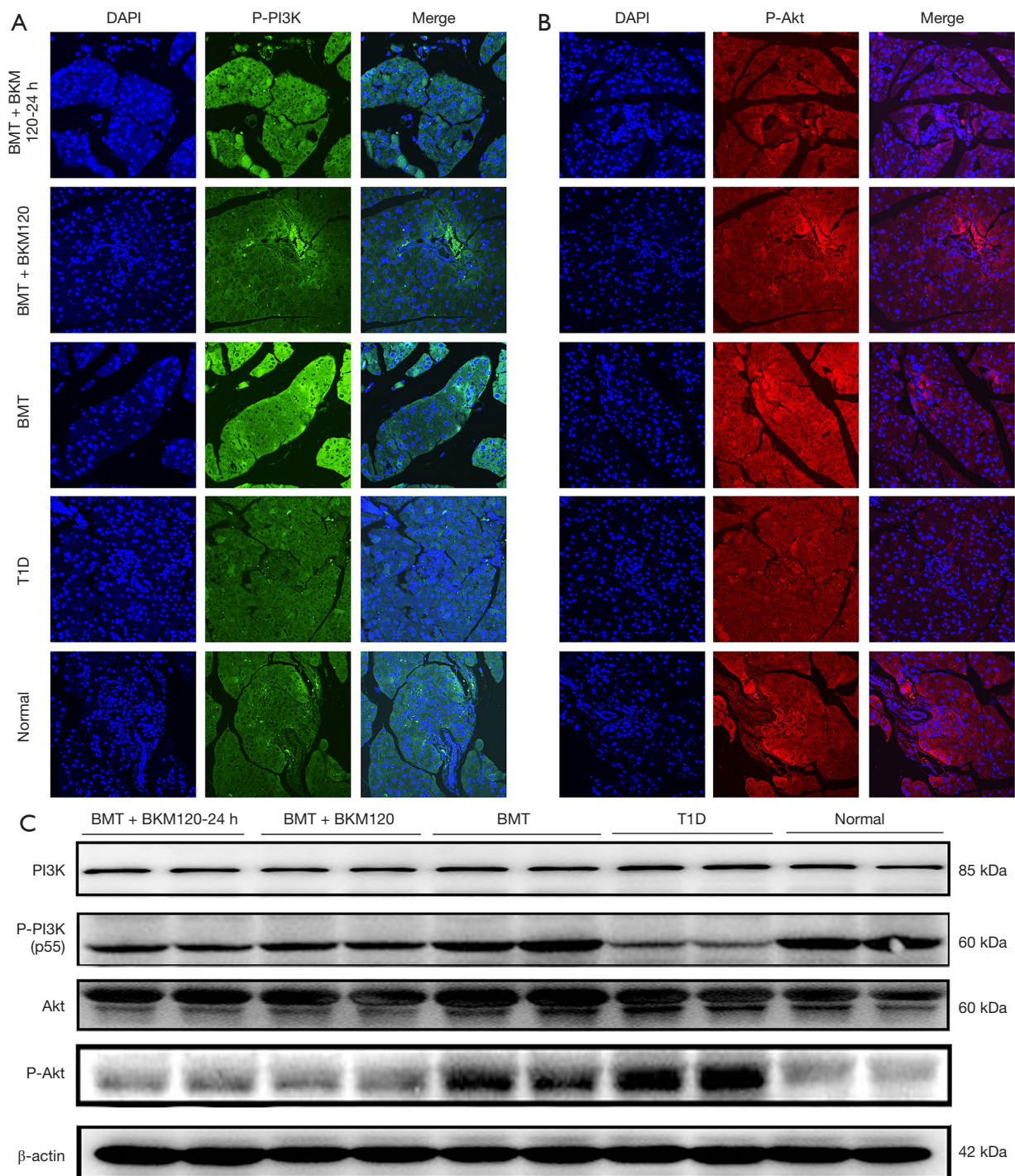
Figure 5 PI3K/Akt signaling pathway was reduced in Treg with BKM120 after syn-BMT. Representative immunofluorescence of (A) P-PI3K and (B) P-Akt in pancreas sections from each group mice (magnification, ×400). (C) Relative protein expression of PI3K, P-PI3K, Akt and P-Akt in CD4⁺CD25⁺ T cells were sorted by MACS from spleens of each group mice. N=6 for each group. *, $P<0.05$; **, $P<0.01$; ***, $P<0.001$; ****, $P<0.0001$. P-PI3K, phospho-phosphoinositide 3-kinases; P-Akt, phospho-protein kinase B; T1D, type 1 diabetes; PI3K, phosphoinositide 3-kinases; Akt, protein kinase B; Treg, regulatory T cell; syn-BMT, syngeneic bone marrow transplantation; MACS, magnetic cell sorting.

Page 12 of 15

Zhang et al. Syngeneic BMT and PI3K inhibitor reversed later-stage T1D

may provide a promising effective therapeutic approach in later-stage T1D.

In this report, we examined the immunoregulatory function of BKM120 on enhancing immune reconstitution after syn-BMT in later-stage STZ-induced T1D. AHSCT rarely reverts hyperglycemia in NOD mice (31), whose spontaneous diabetes is gene mediated. To mimic the AHSCT for T1D in clinic, STZ-induced diabetic mice were used as recipients of syngeneic stem cells. It demonstrated that Akt was abnormally activated in T1D, alongside the ablation of Treg. After syn-BMT in later-stage diabetes, PI3K/Akt signaling was aberrantly activated, along with the aberrant balance of Treg/Th17 and the impaired immunosuppressive function of Treg. BKM120 improved the effects of syn-BMT in controlling blood glucose. It may be that the recovered PI3K/Akt signaling in Treg restored its immunosuppressive function. In addition, BKM120 also controlled Treg/Th17 derangement, which progressively contribute to the amelioration of diabetes.

Interestingly, if BKM120 was only co-cultured with bone marrow cells *in vitro* before syn-BMT, it showed less effectiveness in relieving diabetes and improving immune derangement in recipients. Although activated PI3K/Akt signaling in Treg was also suppressed, the derangement of MDSCs, DCs and Treg, and the impaired Treg's function in recipient was not recovered. Further investigation into the relationship between the Treg's proliferation and its function in T1D is warranted. In addition, while the Treg-maintaining actions of BKM120 were previously reported (14,32), these findings indicate the possibility that additional immunomodulatory mechanisms in recipients may also be at play.

Generally, MDSCs and tolerogenic DCs can effectively inhibit the proliferation of self-reactive and antigraft effector T cells in autoimmunity and transplantation by restraining T-cell activation and promoting Treg expansion (33-35). In allogeneic stem cell transplantation, MDSCs are known to play a potential regulating role in the post-transplant immune environment (36). In contrast, post-AHSCT MDSCs were not associated with 3-year time to progression in patients with multiple myeloma (37). The engagement of MDSCs and DCs in the pathogenesis of T1D is evident as well (38,39). After syn-BMT, we observed a significant increase of Th1 and Th17 cells, alongside a decrease of MDSCs and DCs compared with those in normal control, while the suppressor function of Treg was not well-restored. Moreover, syn-BMT partially suppressed the activation of Akt only in Treg, but not those in pancreas.

These data may, in part, explain insufficient therapeutic efficacy by syn-BMT in later-stage STZ-induced T1D. The restoration of DCs after treatment of BKM120 in combination with syn-BMT may also contribute to the recovery of Treg's function and the amelioration of hyperglycemia.

Achieving effective and durable reversal of T1D is extremely desirable, especially for patients whose treatment was initiated at a later time, as new-onset T1D is rare in clinic. Inhibition of Th17 or blocking IL-17 secretion could delay the development of T1D (40,41). In accordance with our previous report on sarcoidosis (14), BKM120 was found to be effective in rebalancing both Th1/Th2 and Th17/Treg, and restoring Treg's suppressor function in combination with syn-BMT in later-stage STZ-induced T1D. Moreover, BKM120 compensated for the negative effects of syn-BMT on the derangement of Th1/Th2, Th17/Treg and MDSCs/DCs. Worthy of note, ablation and impaired function of Treg, as well as PI3K activation in both pancreas and Treg, which may lead to prolonged disease development, were reversed by BKM120 combined with syn-BMT in recipients. MDSCs/DCs therapy has been shown to promote Treg expansion and induce normoglycemia in murine models of T1D (33,35,42,43). After treatment of BKM120 combined with syn-BMT in later-stage STZ-induced T1D, whether elevated Treg gives a proliferative advantage to MDSCs/DCs, or MDSCs/DCs preferentially expand Treg is under question. However, these data serve as a basis for future PI3K-based immune therapies in combination with stem cell transplantation in later-stage T1D. It should also be noted that only one dosage of BKM120 was used in our study. Whether multiple doses of BKM120 leads to more evident immune tolerance remains an interesting question for future studies.

It may be worthwhile to discuss the targets of BKM120 when it serves as a tolerance-inducing drug. In this study, we have set out to define the differences in the administration of BKM120 that are either through intravenous route into recipients (*in vivo*) or through being cocultured with bone marrow cells (*in vitro*). We noticed that syn-BMT together with intravenous injection of BKM120 successfully maintained normoglycemia. In contrast, if bone marrow cells were only cocultured with BKM120 for 24 h before transplantation, its therapeutic effects were limited, resulting in fluctuated level of glucose after syn-BMT. Both Treg and TGF-β were crucial for MDSCs induction in STZ-treated mice (44). Worthy of note, among our experimental groups, expanded Treg and TGF-β were only

demonstrated in group syn-BMT + BKM120. In group syn-BMT + BKM120-24 h, derangements of Th2 cells, MDSCs and DCs were still noticed. Besides, although activated Akt in Treg was partially suppressed, Treg's function was still impaired after transplantation with BKM120-treated bone marrow cells. These results may be explained by the influence of BKM120 on recipients' micro-environment when BKM120 are used *in vivo* alongside syn-BMT. This hypothesis needs further investigation.

In conclusion, we found that the BKM120 may inhibit the PI3K/Akt signal pathway in the receptor Treg after syn-BMT, enhance Treg's immunosuppressive function, regulate the stability of immune cells, and eventually improve the treatment of syn-BMT in later-stage STZ-induced T1D mice. Targeting PI3K signaling pathway may improve the treatment of syn-BMT for STZ-induced T1D mice by restoring Treg's homeostasis and function. In summary, these results provide vital preclinical data to support the concept of translating PI3K inhibition therapy in combination with AHSCT to patients with later-stage T1D.

Acknowledgments

Footnote

Reporting Checklist: The authors have completed the ARRIVE reporting checklist. Available at https://dx.doi.org/10.21037/atm-21-3329

Data Sharing Statement: Available at https://dx.doi.org/10.21037/atm-21-3329

Conflicts of Interest: All authors have completed the ICMJE uniform disclosure form (available at https://dx.doi.org/10.21037/atm-21-3329). SL, Y Wang, YZ, Y Wen received funding from the Independent and Open Grant of Jiangsu Key Laboratory of Molecular Medicine and Innovation and Entrepreneurship Training Program for College Students (G201910284011). DC, NZ, Y Wen received funding from the Independent and Open Grant of Jiangsu Key Laboratory of Molecular Medicine and Innovation and Entrepreneurship Training Program for College Students (202010284016Z). JD received funding from the National Natural Science Foundation of China (81400046). Y Wen received funding from the National Natural Science Foundation of China (81100386). The other authors have no conflicts of interest to declare.

Ethical Statement: The authors are accountable for all aspects of the work in ensuring that questions related to the accuracy or integrity of any part of the work are appropriately investigated and resolved. All experimental protocols were approved under a project license (SCXK-Jiangsu-2019-0056) granted by Institutional Animal Care and Use Committee of Nanjing University, in compliance with institutional guidelines for the care and use of animals.

References

1. DiMeglio LA, Evans-Molina C, Oram RA. Type 1 diabetes. Lancet 2018;391:2449-62.
2. Pugliese A. Advances in the etiology and mechanisms of type 1 diabetes. Discov Med 2014;18:141-50.
3. Diabetes Control and Complications Trial/Epidemiology of Diabetes Interventions and Complications Research Group; Lachin JM, Genuth S, et al. Retinopathy and nephropathy in patients with type 1 diabetes four years after a trial of intensive therapy. N Engl J Med 2000;342:381-9.
4. Voltarelli JC, Couri CE, Stracieri AB, et al. Autologous nonmyeloablative hematopoietic stem cell transplantation in newly diagnosed type 1 diabetes mellitus. JAMA 2007;297:1568-76.
5. Couri CE, Oliveira MC, Stracieri AB, et al. C-peptide levels and insulin independence following autologous

Page 14 of 15

Zhang et al. Syngeneic BMT and PI3K inhibitor reversed later-stage T1D

nonmyeloablative hematopoietic stem cell transplantation in newly diagnosed type 1 diabetes mellitus. JAMA 2009;301:1573-9.

6. Gu B, Miao H, Zhang J, et al. Clinical benefits of autologous haematopoietic stem cell transplantation in type 1 diabetes patients. Diabetes Metab 2018;44:341-5.

7. Gu W, Hu J, Wang W, et al. Diabetic ketoacidosis at diagnosis influences complete remission after treatment with hematopoietic stem cell transplantation in adolescents with type 1 diabetes. Diabetes Care 2012;35:1413-9.

8. Li L, Shen S, Ouyang J, et al. Autologous hematopoietic stem cell transplantation modulates immunocompetent cells and improves β-cell function in Chinese patients with new onset of type 1 diabetes. J Clin Endocrinol Metab 2012;97:1729-36.

9. Snarski E, Milczarczyk A, Torosian T, et al. Independence of exogenous insulin following immunoablation and stem cell reconstitution in newly diagnosed diabetes type I. Bone Marrow Transplant 2011;46:562-6.

10. D'Addio F, Valderrama Vasquez A, Ben Nasr M, et al. Autologous nonmyeloablative hematopoietic stem cell transplantation in new-onset type 1 diabetes: a multicenter analysis. Diabetes 2014;63:3041-6.

11. Wen Y, Ouyang J, Li W, et al. Time point is important for effects of syngeneic bone marrow transplantation for type 1 diabetes in mice. Transplant Proc 2009;41:1801-7.

12. Wen Y, Ouyang J, Yang R, et al. Reversal of new-onset type 1 diabetes in mice by syngeneic bone marrow transplantation. Biochem Biophys Res Commun 2008;374:282-7.

13. Rocamora-Reverte L, Melzer FL, Würzner R, et al. The Complex Role of Regulatory T Cells in Immunity and Aging. Front Immunol 2021;11:616949.

14. Zhang B, Dai Q, Jin X, et al. Phosphoinositide 3-kinase/protein kinase B inhibition restores regulatory T cell's function in pulmonary sarcoidosis. J Cell Physiol 2019;234:19911-20.

15. Walsh PT, Buckler JL, Zhang J, et al. PTEN inhibits IL-2 receptor-mediated expansion of CD4+ CD25+ Tregs. J Clin Invest 2006;116:2521-31.

16. Sauer S, Bruno L, Hertweck A, et al. T cell receptor signaling controls Foxp3 expression via PI3K, Akt, and mTOR. Proc Natl Acad Sci U S A 2008;105:7797-802.

17. Huynh A, DuPage M, Priyadharshini B, et al. Control of PI(3) kinase in Treg cells maintains homeostasis and lineage stability. Nat Immunol 2015;16:188-96.

18. Pompura SL, Dominguez-Villar M. The PI3K/AKT signaling pathway in regulatory T-cell development,

stability, and function. J Leukoc Biol 2018;103:1065-76.

19. Lim EL, Okkenhaug K. Phosphoinositide 3-kinase δ is a regulatory T-cell target in cancer immunotherapy. Immunology 2019;157:210-8.

20. Fan MY, Turka LA. Immunometabolism and PI(3)K Signaling As a Link between IL-2, Foxp3 Expression, and Suppressor Function in Regulatory T Cells. Front Immunol 2018;9:69.

21. Ouyang W, Liao W, Luo CT, et al. Novel Foxo1-dependent transcriptional programs control T(reg) cell function. Nature 2012;491:554-9.

22. Ouyang W, Beckett O, Ma Q, et al. Foxo proteins cooperatively control the differentiation of Foxp3+ regulatory T cells. Nat Immunol 2010;11:618-27.

23. Kang J, Huddleston SJ, Fraser JM, et al. De novo induction of antigen-specific CD4+CD25+Foxp3+ regulatory T cells in vivo following systemic antigen administration accompanied by blockade of mTOR. J Leukoc Biol 2008;83:1230-9.

24. Merkenschlager M, von Boehmer H. PI3 kinase signalling blocks Foxp3 expression by sequestering Foxo factors. J Exp Med 2010;207:1347-50.

25. Ahmad S, Abu-Eid R, Shrimali R, et al. Differential PI3Kδ Signaling in CD4+ T-cell Subsets Enables Selective Targeting of T Regulatory Cells to Enhance Cancer Immunotherapy. Cancer Res 2017;77:1892-904.

26. Dutra RC, Cola M, Leite DF, et al. Inhibitor of PI3Kγ ameliorates TNBS-induced colitis in mice by affecting the functional activity of CD4+CD25+FoxP3+ regulatory T cells. Br J Pharmacol 2011;163:358-74.

27. Azzi J, Moore RF, Elyaman W, et al. The novel therapeutic effect of phosphoinositide 3-kinase-γ inhibitor AS605240 in autoimmune diabetes. Diabetes 2012;61:1509-18.

28. Maira SM, Pecchi S, Huang A, et al. Identification and characterization of NVP-BKM120, an orally available pan-class I PI3-kinase inhibitor. Mol Cancer Ther 2012;11:317-28.

29. Schultze SM, Hemmings BA, Niessen M, et al. PI3K/AKT, MAPK and AMPK signalling: protein kinases in glucose homeostasis. Expert Rev Mol Med 2012;14:e1.

30. Chi TC, Chen WP, Chi TL, et al. Phosphatidylinositol-3-kinase is involved in the antihyperglycemic effect induced by resveratrol in streptozotocin-induced diabetic rats. Life Sci 2007;80:1713-20.

31. Fiorina P, Voltarelli J, Zavazava N. Immunological applications of stem cells in type 1 diabetes. Endocr Rev 2011;32:725-54.

32. Huijts CM, Santegoets SJ, Quiles Del Rey M, et al.

Differential effects of inhibitors of the PI3K/mTOR pathway on the expansion and functionality of regulatory T cells. Clin Immunol 2016;168:47-54.

33. Yin B, Ma G, Yen CY, et al. Myeloid-derived suppressor cells prevent type 1 diabetes in murine models. J Immunol 2010;185:5828-34.

34. Min WP, Zhou D, Ichim TE, et al. Inhibitory feedback loop between tolerogenic dendritic cells and regulatory T cells in transplant tolerance. J Immunol 2003;170:1304-12.

35. Zoso A, Mazza EM, Bicciato S, et al. Human fibrocytic myeloid-derived suppressor cells express IDO and promote tolerance via Treg-cell expansion. Eur J Immunol 2014;44:3307-19.

36. Zhang Q, Fujino M, Xu J, et al. The Role and Potential Therapeutic Application of Myeloid-Derived Suppressor Cells in Allo- and Autoimmunity. Mediators Inflamm 2015;2015:421927.

37. Lee SE, Lim JY, Kim TW, et al. Different role of circulating myeloid-derived suppressor cells in patients with multiple myeloma undergoing autologous stem cell transplantation. J Immunother Cancer 2019;7:35.

38. Grohová A, Dáňová K, Adkins I, et al. Myeloid - derived suppressor cells in Type 1 diabetes are an expanded population exhibiting diverse T-cell suppressor mechanisms. PLoS One 2020;15:e0242092.

39. Calderon B, Suri A, Miller MJ, et al. Dendritic cells in islets of Langerhans constitutively present beta cell-derived peptides bound to their class II MHC molecules. Proc Natl Acad Sci U S A 2008;105:6121-6.

40. Emamaullee JA, Davis J, Merani S, et al. Inhibition of Th17 cells regulates autoimmune diabetes in NOD mice. Diabetes 2009;58:1302-11.

41. Jain R, Tartar DM, Gregg RK, et al. Innocuous IFNgamma induced by adjuvant-free antigen restores normoglycemia in NOD mice through inhibition of IL-17 production. J Exp Med 2008;205:207-18.

42. Funda DP, Palová-Jelínková L, Goliáš J, et al. Optimal Tolerogenic Dendritic Cells in Type 1 Diabetes (T1D) Therapy: What Can We Learn From Non-obese Diabetic (NOD) Mouse Models? Front Immunol 2019;10:967.

43. Lee M, Kim AY, Kang Y. Defects in the differentiation and function of bone marrow-derived dendritic cells in non-obese diabetic mice. J Korean Med Sci 2000;15:217-23.

44. Gao X, Liu H, He B, et al. Resistance to Streptozotocin-Induced Autoimmune Diabetes in Absence of Complement C3: Myeloid-Derived Suppressor Cells Play a Role. PLoS One 2013;8:e66334.